

## Wide Band First Shear Horizontal Mode Plate Wave Resonator on 175° YX LiNbO<sub>3</sub> Thin Plate

Ferriady Setiawan<sup>1\*</sup>, Michio Kadota<sup>2</sup>, and Shuji Tanaka<sup>3</sup> (<sup>1</sup>Grad. School Eng., Tohoku Univ.)

### 1. Introduction

High-frequency and wide-bandwidth acoustic wave devices have been investigated for 5G and beyond 5G communication. 5G new bands of n77, n78, and n79 require a bandwidth ( $BW$ ) as wide as 27%, 15%, and 13%, respectively.<sup>1)</sup> Plate wave resonators using the first anti-symmetric mode ( $A_1$ ) and its higher mode, as well as the first shear horizontal mode ( $SH_1$ ), have been studied to overcome the limitations of surface acoustic wave (SAW) and bulk acoustic wave (BAW) devices.<sup>2-5)</sup> Thin BAW resonators (FBAR) using ScAlN have been studied for wideband filters.<sup>6)</sup> However, excessive Sc doping increases its dielectric loss. An  $SH_1$  mode resonator on a 0.5  $\mu\text{m}$  thick LiTaO<sub>3</sub> (LT) thin plate exhibited a frequency of 2.82 GHz, but it had a narrow  $BW$  of 3.8%.<sup>7)</sup> A 3.23 GHz  $SH_1$  mode resonator on a LiNbO<sub>3</sub> (LN) thin plate was studied by Kadota *et al.* However, the resonator had stray capacitance and parasitic inductance, which limited its frequency characteristics.<sup>8)</sup>

This paper reports a high-frequency  $SH_1$  mode resonator on an LN thin plate using an isolated bottom electrode to avoid stray capacitance and parasitic inductance. The aim is to demonstrate wideband acoustic devices for 5G new bands.

### 2. Phase Velocity and Coupling Factor Simulation by FEM

**Figs. 1 and 2** show the phase velocity and coupling factor ( $k^2$ ) of the  $SH_1$  mode resonator on an LN thin plate with a thickness of  $0.1\lambda$  (wavelength) as a function of the second Euler angle  $\theta$ . The  $SH_1$  mode on  $(0^\circ, 85^\circ, 0^\circ)$  LN exhibits a high phase velocity of more than 20 km/s and a high  $k^2$  of 36%. This high  $k^2$  is achieved by making the bottom LN plane (opposite to the IDT side) electrically shorted, as reported in Ref. 7 and 8. **Figs. 3 and 4** show the simulated phase velocities and  $BW$  of different modes on  $(0^\circ, 85^\circ, 0^\circ)$  LN as the normalized thickness varies, respectively. The red solid line represents the simulated phase velocity and  $BW$  in case of using an 80 nm thick Al IDT with a metallization ratio ( $MR$ ) of 0.8. Notably, the phase velocity of the  $SH_1$  mode decreases significantly as the LN thickness exceeds  $0.1\lambda$ . The  $BW$  also increases as the LN normalized thickness becomes

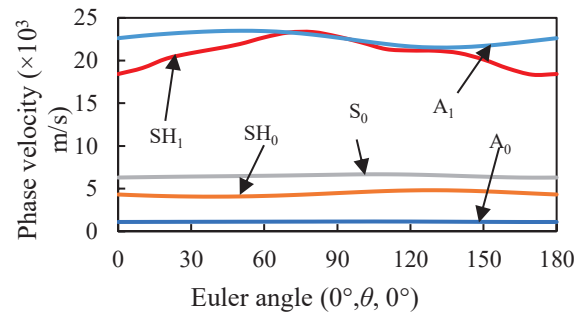


Fig. 1 Phase velocity of various modes of plate waves on LN with  $0.1\lambda$  thickness as a function of Euler angle  $(0^\circ, \theta, 0^\circ)$ .

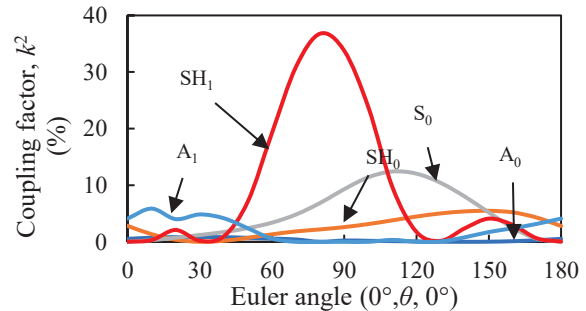


Fig. 2 Coupling factor ( $k^2$ ) of various modes of plate waves on  $0.1\lambda$  thick LN with electrically shorted bottom plane as a function of angle  $(0^\circ, \theta, 0^\circ)$ .

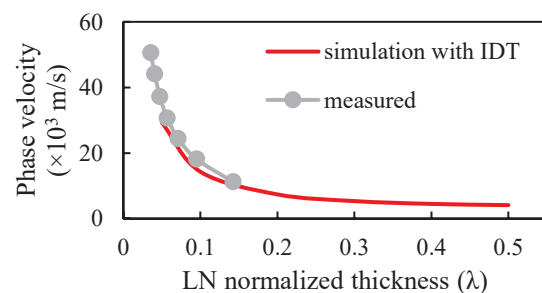


Fig. 3 Phase velocity of  $SH_1$  mode on  $(0^\circ, 85^\circ, 0^\circ)$  LN with electrically shorted bottom plane as a function of LN normalized thickness.

smaller.

### 3. Fabrication and Measurement

The  $SH_1$  mode resonator was fabricated on a 0.57  $\mu\text{m}$  thick  $(0^\circ, 85^\circ, 0^\circ)$  LN thin plate. The IDT  $\lambda$  was designed to be between 4-16  $\mu\text{m}$  with a thickness of 80 nm using Al as an electrode material to achieve higher frequency. A  $MR$  of 0.8 was chosen to eliminate the electric field in the planar direction.

E-mail: <sup>\*</sup>setiawan.ferriady.r1@dc.tohoku.ac.jp

The supporting Si wafer was etched from the backside to create a suspended LN plate. To prevent stray capacitance due to metal connecting between LN and Si side walls, the backside etching was performed in two steps, firstly, anisotropic deep reactive ion etching (DRIE) for 180  $\mu\text{m}$  depth, and secondly, isotropic plasma etching for additional 50  $\mu\text{m}$  depth to make overhanging structures. Finally, an 80 nm thick Al was deposited to form the electrically short bottom plane. **Fig. 5 (a)** shows the cross-section structure of the SH<sub>1</sub> mode resonator, and **Fig. 5 (b)** is the top view of the fabricated SH<sub>1</sub> mode resonator.

**Fig. 6** shows one of the frequency characteristics of the fabricated SH<sub>1</sub> mode resonator measured using Keysight's E5071C Network Analyzer. The main response includes some spurious responses, which come from the thickness shear (TS) mode bulk wave which might also be excited by using the IDT with a *MR* of 0.8. A resonance frequency ( $f_r$ ) of 2.57 GHz, an anti-resonance frequency ( $f_a$ ) of 3.07 GHz, a wide *BW* of 19.5%, and an impedance (*Z*) ratio of 30.5 dB were measured.

Measured phase velocities and *BWs* are shown with dots in Figs. 3 and 4. The measured phase velocities are close to the simulated ones, which confirms that the main response was SH<sub>1</sub> mode plate wave, because the bulk wave velocity remains constant regardless of the LN thickness. The measured *BWs* are far from simulated ones because the in-band spurious response might affect the  $f_r$  and  $f_a$ . Nevertheless, the trend was similar; the *BW* increases as the LN normalized thickness becomes larger ( $\lambda$  becomes larger). Higher frequencies can be achieved by further thinning the LN plate. The spurious-free resonator will be studied in future improvements.

#### 4. Conclusion

This study investigated the wide *BW* characteristics of the SH<sub>1</sub> mode resonator on thin LN with Al as the IDT and backside electrode. The fabrication process incorporates a technique to eliminate stray capacitance and inductance influences. A frequency around 3 GHz and *BW* of 19% were reported, making it suitable for 5G new bands. A wider *BW* was observed as  $\lambda$  increased, attributable to larger LN normalized thickness. Future improvements aim to achieve a higher *Z* ratio and spurious-free frequency characteristic.

#### Acknowledgment

This research was partly supported by SCOPE #JP225002001. We would like to thank Dr. Hideki Takagi at the National Institute of Advanced Industrial Science and Technology (AIST) for the bonding of the wafers and Prof. Kenya Hashimoto

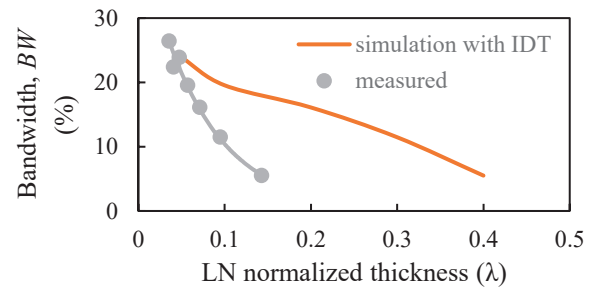


Fig. 4 Bandwidth (*BW*) of SH<sub>1</sub> mode on (0°, 85°, 0°) LN with electrically short bottom plane as a function of LN normalized thickness.

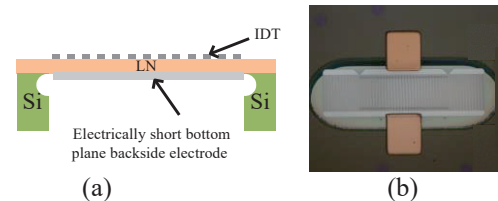


Fig. 5 Structure of fabricated SH<sub>1</sub> mode resonator. (a) Cross section and (b) Top view.

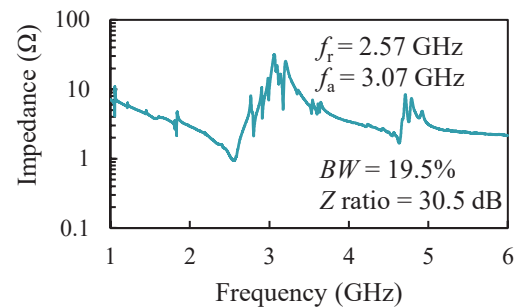


Fig. 6 Measured frequency characteristic of fabricated SH<sub>1</sub> mode resonator on LN thin plate.

at University of Electronic Science and Technology of China for useful discussion.

#### References

- 1) Adding channel bandwidth to existing NR bands, <https://www.3gpp.org/technologies/adding-channel-bandwidth-to-existing-nr-bands> (accessed in August 2023).
- 2) M. Kadota, T. Ogami, K. Yamamoto, H. Tochishita and Y. Negoro: IEEE Trans. Ultrason. Ferroelectr. Freq. Contr., 57 (2010) 2564.
- 3) M. Kadota and T. Ogami: Jpn. J. Appl. Phys. 50 (2011) 07HD11.
- 4) N. Assila, M. Kadota and S. Tanaka: IEEE Trans. Ultrason. Ferroelectr. Freq. Contr., 66 (2019) 1529.
- 5) Y. Yang, R. Lu, L. Gao and S. Gong: IEEE Trans. Microw. Theory Tech., 68 (2020) 5211.
- 6) M. Moreira, J. Bjurstrom, I. Katardjev, V. Yantchev: Vacuum, 86 (2011) 23.
- 7) M. Kadota, S. Tanaka and T. Kimura: Proc. IEEE Int. Ultrason. Symp. 2015, P4B1-5-1.
- 8) F. Setiawan, M. Kadota and S. Tanaka: Proc. IEEE Int. Ultrason. Symp. 2021, B3L-05-02.